

SERVing up Clustering Around Obscured and Unobscured Quasars at $z=1\sim 2$



K.M. Jones^{1,2,4} Mark Lacy² D. Nielsen³, the SERVS team

1: Arecibo Observatory 2: National Radio Astronomy Observatory 3: University of Wisconsin-Madison 4: University of Virginia



Results

Why Study Obscured Quasars?

IMPORTANCE FOR THE FIELD:

- quasar population + transport of gas/momentum = massive galaxy evolution
- galaxy evolution (+role quasars play) may change at different z
- quasars have $L_{\text{nuc}} > L_{\text{host}}$, so hosts also understudied
- Surveys (see, i.e., Lacy+15, accepted) have determined that obscured quasars make up on order of 50% of the total quasar population. This indicates that previous research on quasars, which has focused primarily on optical quasars, is biased--it investigates only a portion of the total population. Study of obscured quasars is necessary to fully understand the role that SMBH play in the evolution of galaxies.
- Optical quasars are so bright that they completely blot out the host galaxy in which they are embedded. Obscured quasars are sufficiently shrouded to allow their hosts to be seen, allowing one to study the relation between a supermassive black hole and the host galaxy.

Type	$A_{\text{gg}} \times 10^{-3}$ ($\text{rad}^{0.77}$)	$\sigma \times 10^{-3}$ ($\text{rad}^{0.77}$)	$SE_x \times 10^{-3}$ ($\text{rad}^{0.77}$)
Type 1 QSOs	0.24	0.30	0.066
Type 1 QSOs (no outlier)	0.18	0.16	0.037
Type 2 Quasars (obscured)	0.21	0.12	0.028
Type 1R QSOs	0.30	0.14	0.052

Table 1: Average angular cross-correlation amplitude results for the different quasar types.

Measuring Environmental Richness

- Quasars not necessarily in virialized clusters
 - but are in regions of greater-than-average number density
- How?
 - Calculate richness via cross-correlation (e.g. various, from Longair & Seldner (1979) to Donoso et al. 2014 and Allevalo et al. 2014)
- Sample galaxies selected from the Spitzer Extragalactic Representative Volume Survey (SERVS) (see, e.g., Mauduit, et al 2012).
 - This is an 18 deg² survey to the depth of 23.1 AB magnitude or $\sim 2\mu\text{Jy}$ at 3.6 and 4.5 microns.
 - It overlaps with five astronomical fields with complementary data and observations available (ELAIS-N1, ELAIS-S1, Lockman Hole, Chandra Deep Field South, XMM-LSS).
 - SERVS is deep enough, and covers sufficient z , to offer a statistically significant number of galaxies to study.
- Galaxy selection: in the manner described in Falder, et al. 2011; see their Fig 3 or our Fig 1. below.
- Supplementary data available: SERVS overlaps with near-infrared datasets such as UKIDSS (Lawrence, et al. 2007) and VIDEO (Jarvis, et al. 2013), allowing accurate redshift determinations.

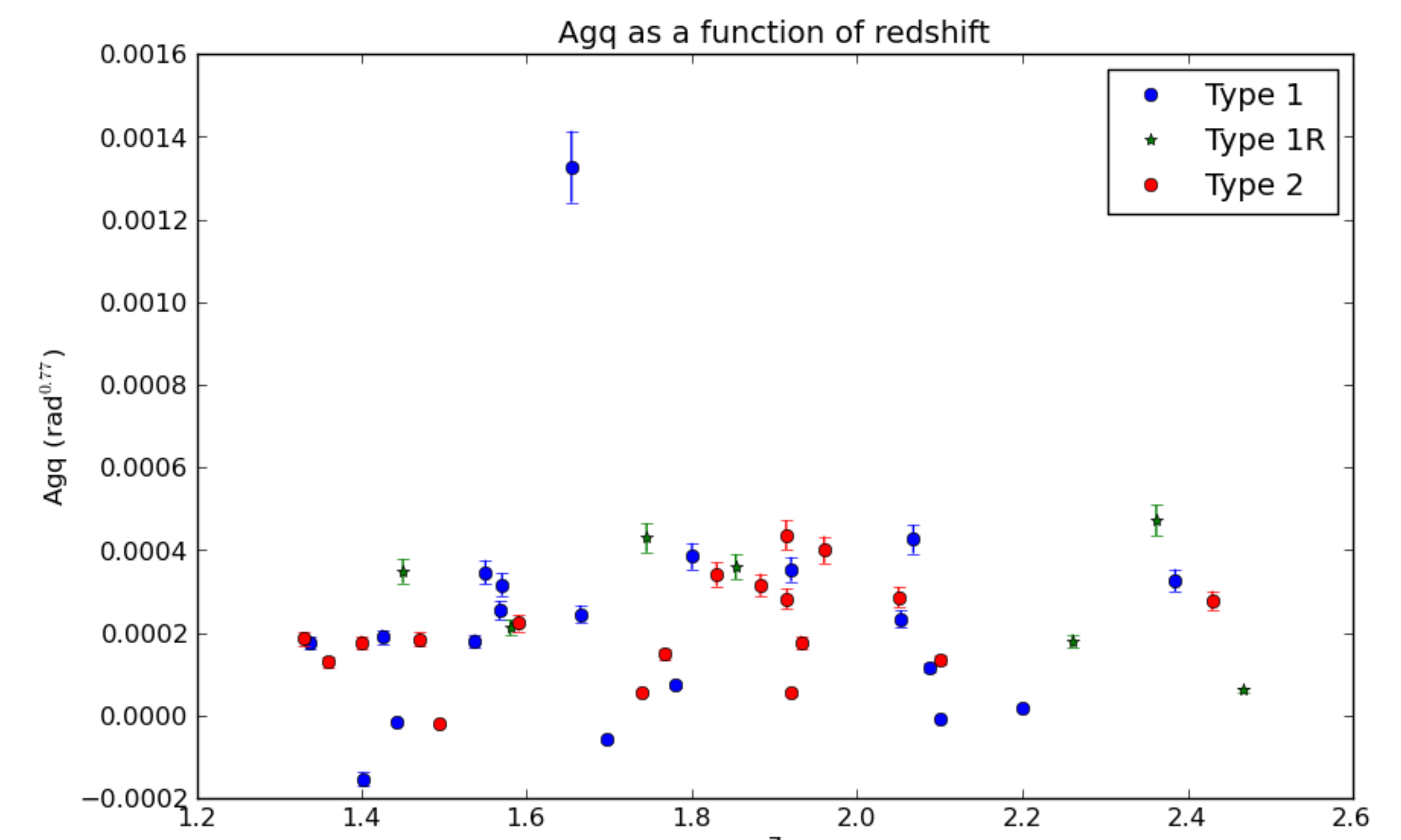


Fig 2: Angular cross-correlation amplitude results as a function of redshift, with relative errors. Note the Type 1 outlier with an A_{gg} of ~ 0.0013 (see images below). Note also there is no clear dependence on redshift.

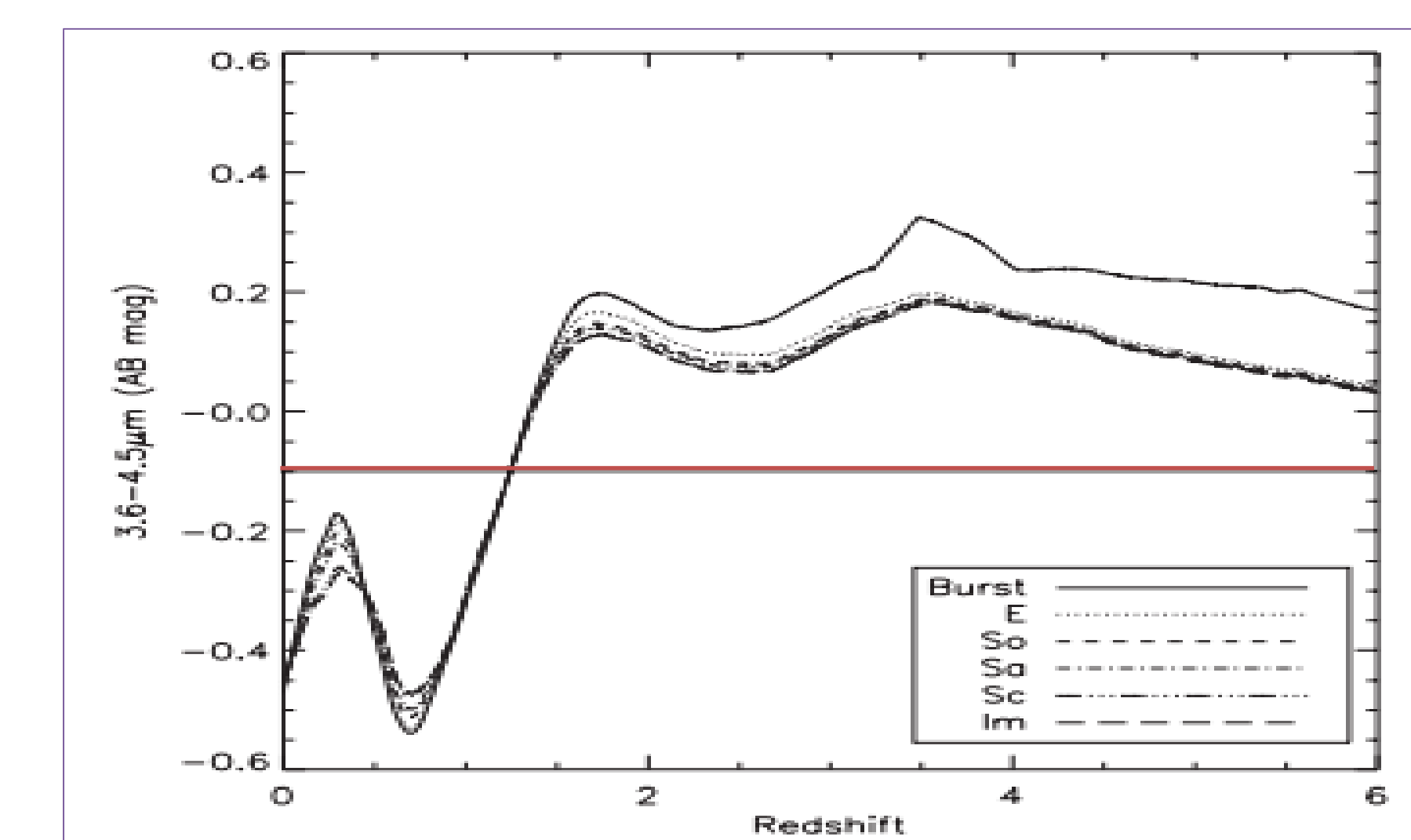


Fig 1. from Falder, et al. (2011). Models of 3.6-4.5 um color as a function of z for different stellar populations/galaxy types. We use a color selection of $[3.6]-[4.5] > -0.1$ (red line)

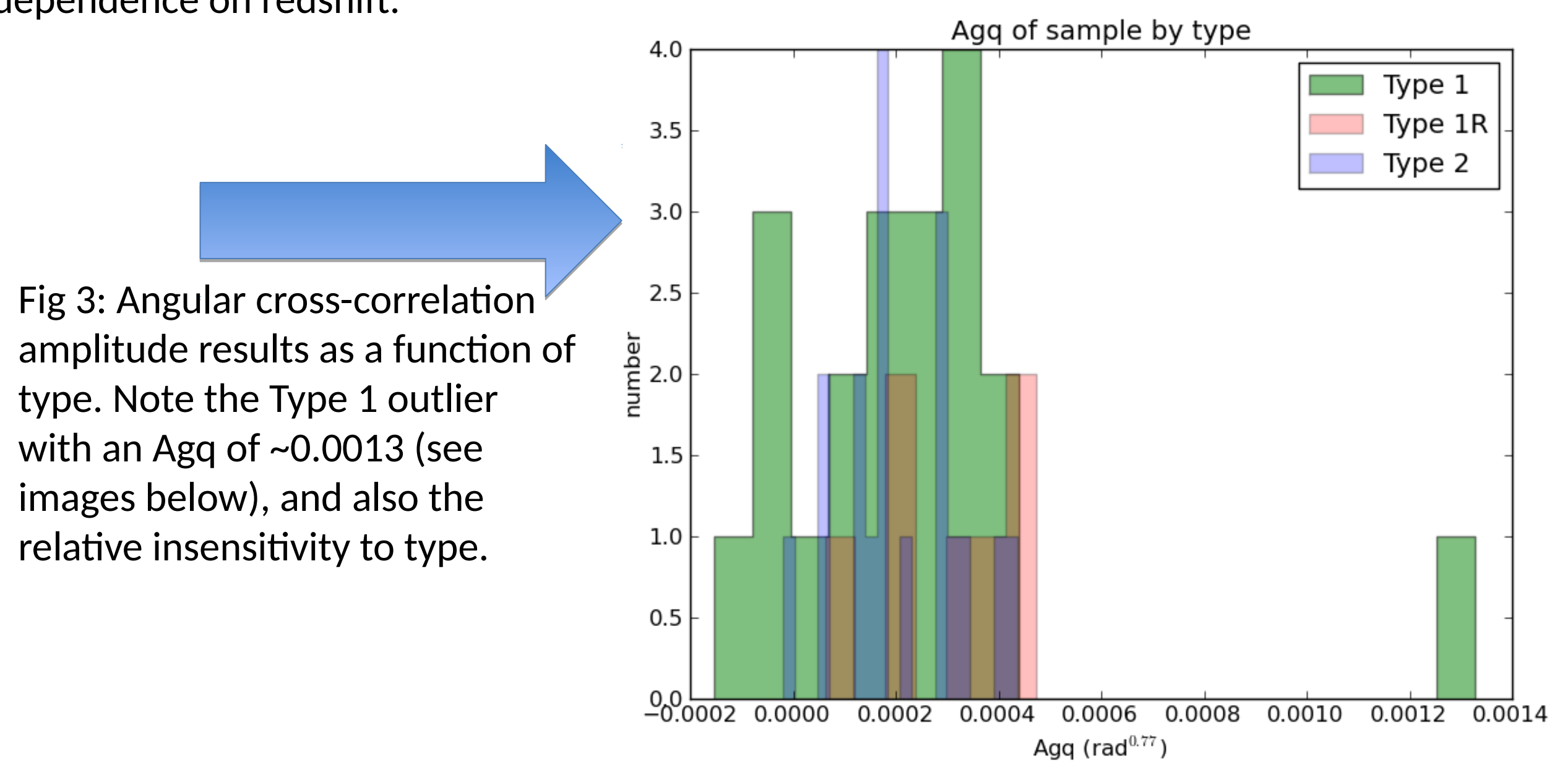


Fig 3: Angular cross-correlation amplitude results as a function of type. Note the Type 1 outlier with an A_{gg} of ~ 0.0013 (see images below), and also the relative insensitivity to type.

Clustering Measurements

- Angular Cross Correlation Function:

$$\omega(\theta) = A_{\text{gg}} \theta^{1-\gamma}$$
- A_{gg} measurements
 - Depends on background subtraction, z , and J
- We follow Wold+Lacy 00 and approximate J to get:

$$A_{\text{gg}} = \frac{N_{\text{tot}} - N_b}{N_b} \frac{3 - \gamma}{2} \theta^{\gamma-1}$$

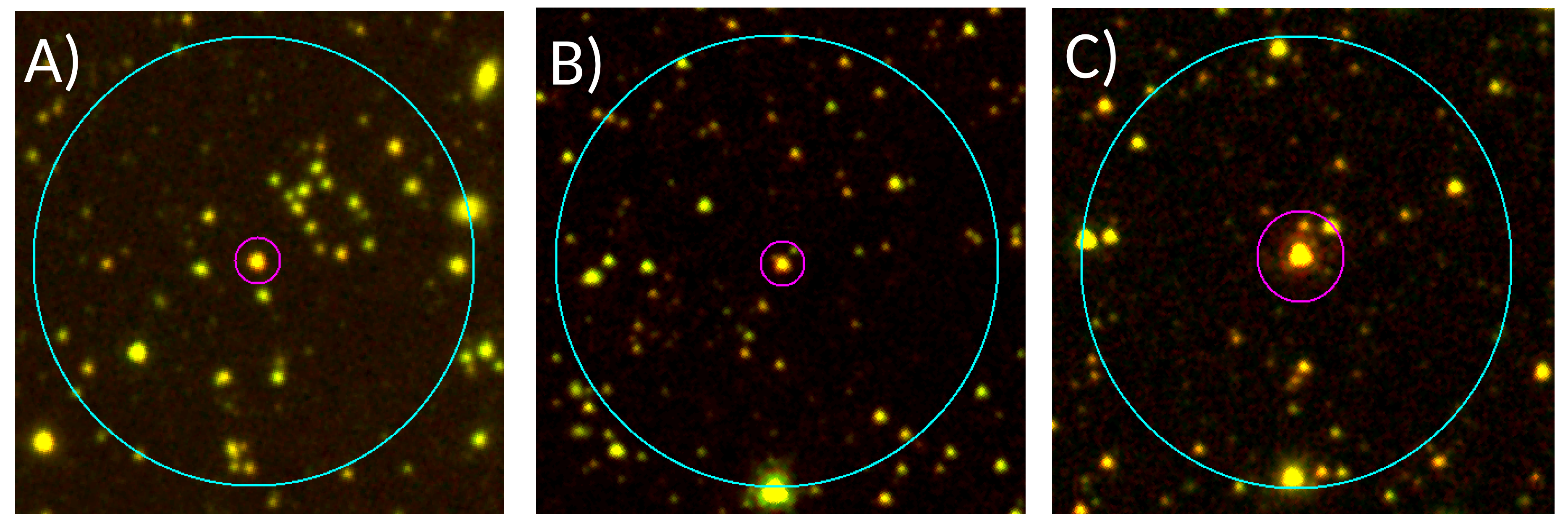


Fig 4. Sample Spitzer fields of our objects. Green is IRAC band 3.6 μm ; red is IRAC band 4.5 μm . Blue, if present, is UKIDSS K-Band. The magenta circle indicates the quasar and the cyan circle indicates a radius of 0.5 Mpc at the given redshift. A) A spectroscopically confirmed Type 1 QSO (SW021902.58-044628.4) with a low $A_{\text{gg}} \sim 5.7 \times 10^{-5}$. B) A spectroscopically confirmed Type 2 quasar (SW105531.79+572714.9) with an average $A_{\text{gg}} \sim 3.2 \times 10^{-4}$. C) A spectroscopically confirmed Type 1 QSO (SW105447.29+581909.4) with an unusually high $A_{\text{gg}} \sim 1.3 \times 10^{-3}$

QUASAR SELECTION:

Traditional quasar identifiers (e.g. Schmidt (1969)):

- Blue continuum from high UV flux
- Broad emission lines (i.e. H- α , H- β , Ly- α , Mg II, CIV)

Type-2 quasar challenges:

- Complete obscuration of broad lines
- Dust reddening of continuum

Identification method (e.g. Lacy, et al (2013), Stern, et al (2005), Lacy, et al (2004)):

- MIR color-slice (see Fig 3)
- Follow-up optical spectroscopy (e.g. Fig 4)

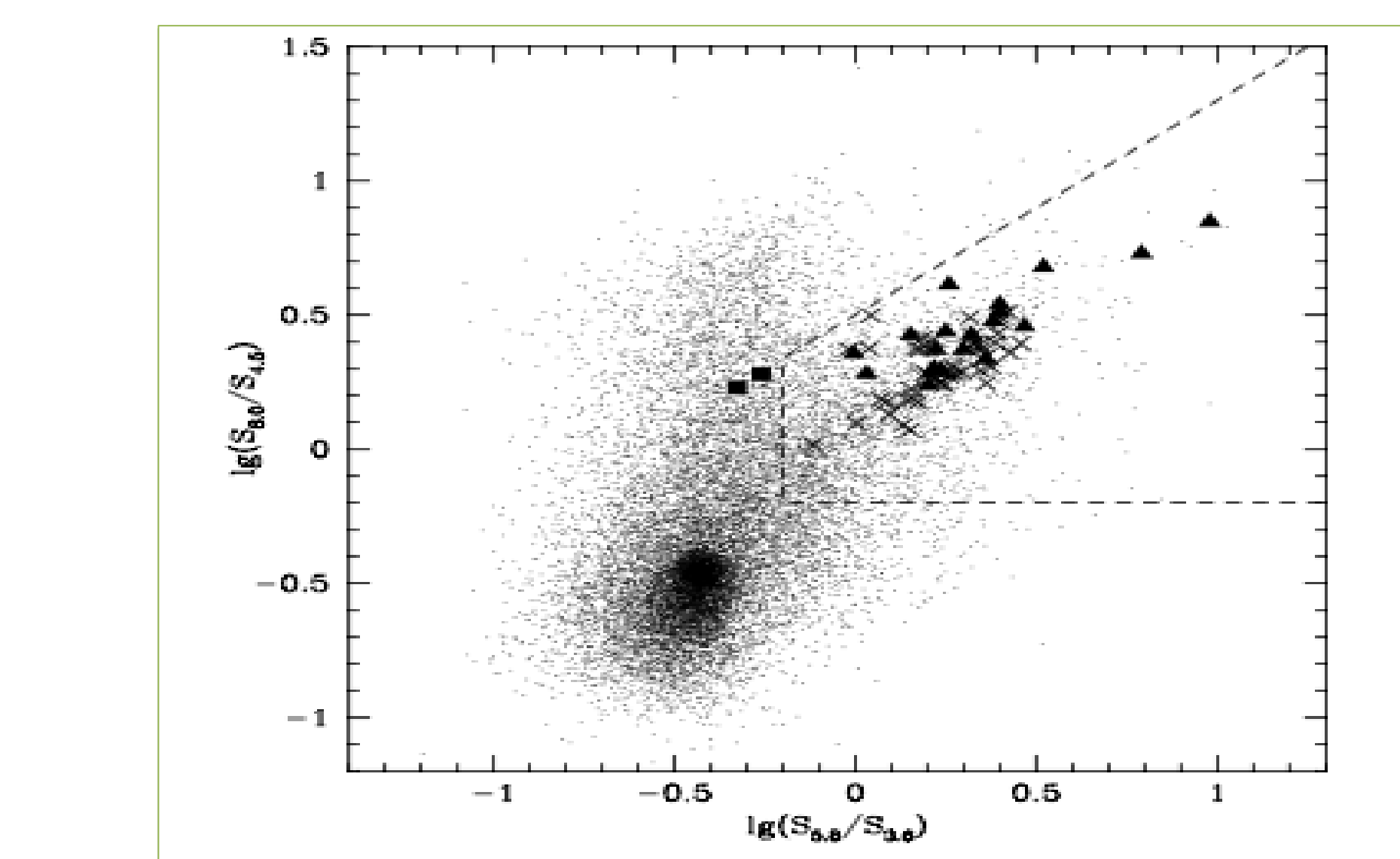


Fig 5. from Lacy, et al. (2004). 54 known SDSS quasars identify the Lacy Wedge, a MIR color-space selection for quasars. Dots are SDSS objects with clean IRAC detections; triangles are bright obscured AGN; crosses are SDSS and radio-identified quasars; squares are SDSS Seyfert 1

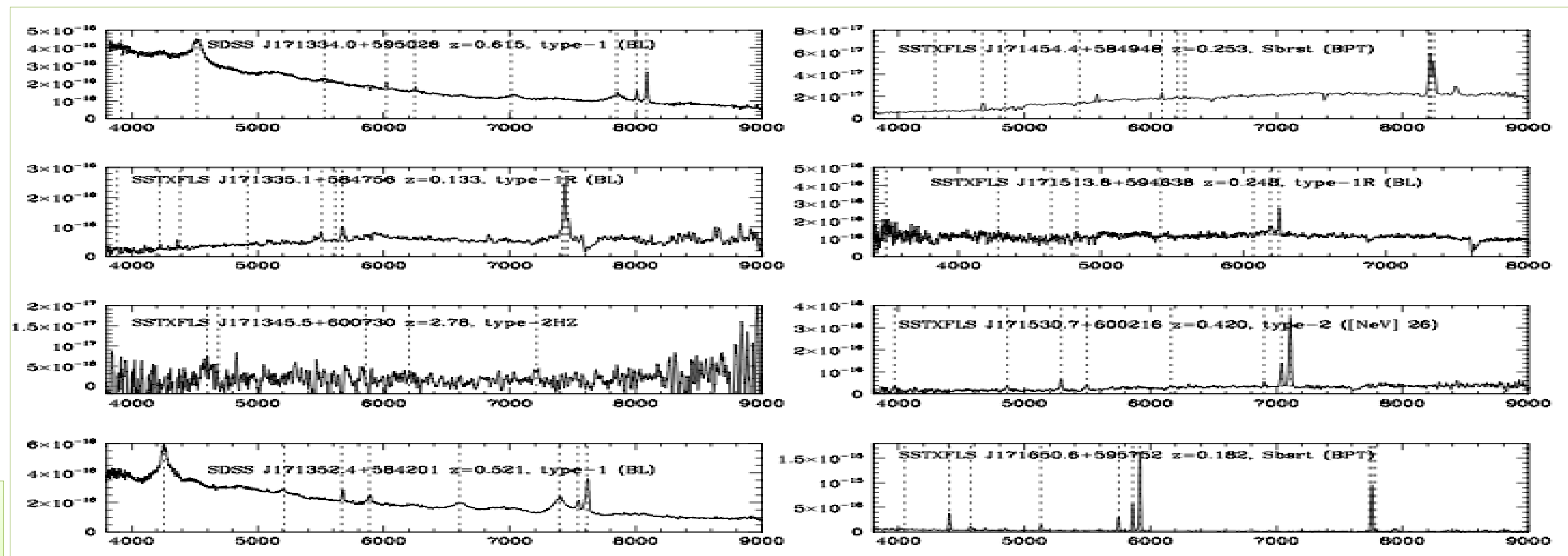


Fig 6. from Lacy, et al. (2007). Example spectra and their identifications. Dashed vertical lines indicate detected emission lines

Quasar identification results (Lacy, et al (2013), $z \approx 0 - 3$; 527/672 total identified objects are AGN):

- Type 1 quasars, with broad lines and a blue continuum (137) (for this study, 20)
- Type 1R quasars, with broad lines but no blue continuum (96) (for this study, 7)
- Type 2 quasars, with high ionization narrow emission lines that could not be produced by pure starburst alone (from SB modeling) (294) *for this study, 18)